Available online at www.sciencedirect.com
SCIENCE DIRECT®
Journal of Chromatography A, 1090 (2005) 39–57
JOURNAL OF CHROMATOGRAPHY A
www.elsevier.com/locate/chroma

Separation mechanism of nortriptyline and amytriptyline in RPLC

Fabrice Gritti[a], Georges Guiochon[b,*]

[a] *Department of Chemistry, University of Tennessee, Knoxville, TN 37996-1600, USA*
[b] *Division of Chemical Sciences, Oak Ridge National Laboratory, Oak Ridge, TN 37831-6120, USA*

Received 28 January 2005; received in revised form 16 June 2005; accepted 22 June 2005
Available online 10 August 2005

Abstract

The single and the competitive equilibrium isotherms of nortriptyline and amytriptyline were acquired by frontal analysis (FA) on the C_{18}-bonded discovery column, using a 28/72 (v/v) mixture of acetonitrile and water buffered with phosphate (20 mM, pH 2.70). The adsorption energy distributions (AED) of each compound were calculated from the raw adsorption data. Both the fitting of the adsorption data using multi-linear regression analysis and the AEDs are consistent with a trimodal isotherm model. The single-component isotherm data fit well to the tri-Langmuir isotherm model. The extension to a competitive two-component tri-Langmuir isotherm model based on the best parameters of the single-component isotherms does not account well for the breakthrough curves nor for the overloaded band profiles measured for mixtures of nortriptyline and amytriptyline. However, it was possible to derive adjusted parameters of a competitive tri-Langmuir model based on the fitting of the adsorption data obtained for these mixtures. A very good agreement was then found between the calculated and the experimental overloaded band profiles of all the mixtures injected.

Keywords: Adsorption equilibrium; Single and competitive adsorption isotherms; Frontal analysis; Column heterogeneity; Affinity energy distribution; Retention mechanism; Preparative chromatography; Silica; Discovery-C_{18}; Nortriptyline; Amytriptyline; Acetonitrile

1. Introduction

Reversed phase liquid chromatography (RPLC) is now the most widely applied technique to perform analytical or preparative separations of mixtures of pharmaceutical, biological, environmental, or food interest. It is used with neutral and with ionizable compounds. A better understanding of the retention mechanism of RPLC is required in order better to optimize the speed and cost of analyses and/or production of the components of interest. Two opposite approaches can be used to achieve this goal. The empirical and pragmatic methods commonly employed are based on the acquisition of a minimum number of experimental results and on an optimization of the experimental conditions made using a dedicated chromatographic software. This method does not require, however, any fundamental understanding of the adsorption mechanism of the compounds studied. An alternative method consists in trying and understanding the effects of the experimental parameters on the adsorption of the eluites in order to predict accurately their chromatographic band profile [1]. The measurement of the single-component adsorption isotherms of the compounds of interest on various C_{18}-bonded silica adsorbents as a function of the temperature [2], the pressure [3], the mobile phase composition (nature and concentration of the organic modifier [4], ionic strength [5–8] and nature of the buffer [9,10]) has already been experimentally investigated in RPLC. All these results give important insights on the retention mechanisms involved. Yet, all these studies have neglected a particular aspect of the adsorption problem, the degree of heterogeneity of the adsorbent surface, because its quantification was impractical until very recently. Yet, we begin to realize that this aspect is critical whenever column overloading is considered, whether for trace analyses of for the extraction or purification of certain chemicals.

The degree of heterogeneity of an adsorbent surface seems to be a parameter of great fundamental importance in the

* Corresponding author. Tel.: +1 865 974 0733; fax: +1 865 974 2667.
E-mail address: guiochon@utk.edu (G. Guiochon).

0021-9673/$ – see front matter © 2005 Elsevier B.V. All rights reserved.
doi:10.1016/j.chroma.2005.06.079

RPLC separation process. As a matter of fact, the surface of no conventional RPLC stationary phase is homogeneous [11]. Of particular significance is the heterogeneity of the C_{18}-bonded layer structure. The importance of this characteristic has been suggested independently by the results of solid-state nuclear magnetic resonance measurements [12]. These data suggest that this structure involve very regular domains in which the bonded alkyl chains are regularly arranged and domains in which the chains are nearly as randomly organized as in a liquid. Earlier nonlinear chromatographic work suggests the coexistence on the surface of most C_{18}-bonded silica adsorbents of several types of sites, usually two or three. The adsorption energy distributions of these stationary phases exhibit several very narrow modes, with markedly different average adsorption constants. Each type is nearly homogeneous but the coexistence of several types of sites has nefarious consequences. Adsorption takes place first on the highest energy sites, on which the adsorption constant is largest. Unfortunately, these sites have a rather low saturation capacity. Because the band profiles become unsymmetrical and their retention times begin to vary with increasing sample size as soon as this size reaches a few percents of the saturation capacity of this type of sites, the analysis of traces is difficult. The maximum sample size which can be used in practice is limited by the saturation capacity of the high energy sites, not by that of the low-energy sites that is between two and three orders of magnitude larger. These problems have been identified and illustrated recently [13].

The goal of this work was to investigate the consequences of the heterogeneity of the surface of packing materials made of C_{18}-bonded silica in preparative chromatography. Sample sizes used are much larger, concentrations are not in the range of onset of overloading, at the border of the linear range, but well inside the nonlinear range of concentrations where the isotherm curvature is significant. This study should involve the separation of two compounds and we chose for that amitriptylline and nortriptylline. The prediction of the exact position and shape of overloaded chromatographic band profiles is easily done provided the correct competitive adsorption isotherms are available [1,14]. Competitive isotherms have been less aggressively studied than single-component isotherms and the modeling of the competition between several compounds for access to the adsorbent surface is still a challenging problem. The determination of the single-component isotherms of the feed components is a first step in this endeavor and the best models of single-component adsorption data are generally used as building blocks for the competitive adsorption isotherms of the mixture. In trace analyses, the band profiles are nearly symmetrical and independent of the sample composition when the concentration of the corresponding compound is small and $b_{\max,i}C_i \ll 1$, where $b_{\max,i}$ is the highest equilibrium constant between the liquid and the solid phase, as derived from the adsorption energy distribution of the modeling of the adsorption data. In preparative chromatography, however, the concentrations used are much larger, the bands overlap and the prediction of their profiles is possible only when the competitive isotherm of each feed component is accurately known.

As a first approximation, multi-component competitive isotherms can be derived from the single-component isotherms of the corresponding compounds using the corresponding classical models of competitive isotherms [1]. Whenever it applies, this approach avoids the long and laborious measurements of competitive adsorption data. Unfortunately, deviations of the experimental competitive adsorption data from the predictions of the competitive isotherm models derived from the extension of the single-component models are frequent and often important. In the best cases, some adjustment of the isotherm parameters may be required. Thus, the acquisition of some experimental data remains necessary. As we explain later, frontal analysis [15,16] is the most accurate method to measure competitive isotherm data. It is straightforward to apply only in the case of two components that exhibit a langmuirian isotherm behavior, i.e., a breakthrough curve with front shock layers and diffuse rear boundaries. Alternately, the perturbation method on the plateau is used [17].

In this work, we measured by frontal analysis the single-component and the competitive adsorption isotherm data of nortriptyline and amytriptyline, two aromatic amines with very similar molecular structures that are used as antidepressants, on a C_{18}-bonded silica adsorbent. Validation of the competitive isotherm model was done by comparing the calculated and the experimental overloaded band profiles of mixtures of the two compounds.

2. Theory

2.1. Determination of the adsorption isotherms

The single-component and competitive adsorption isotherms were measured by the dynamic frontal analysis method. This method is described elsewhere [1]. It is time consuming but gives accurate data. In the case of single-component isotherm data, the amounts adsorbed at equilib-

Table 1
Physico-chemical properties of the Discovery-C_{18} adsorbent material packed in a stainless steel tube (150 mm × 4.0 mm)

Particle shape	Spherical
Particle size (μm)	5
Pore size (Å)	180
Specific surface (m^2/g) (before derivatization)	200
Total carbon (%)	12
Surface coverage (μmol/m^2)	3.0
Endcapping	YES
Void volume measurements	1.363[a]
	1.378[b]
	1.349[c]

[a] Elution of unretained compound method.
[b] Minor disturbance method.
[c] Pycnometry method (ACN-CH_2Cl_2).

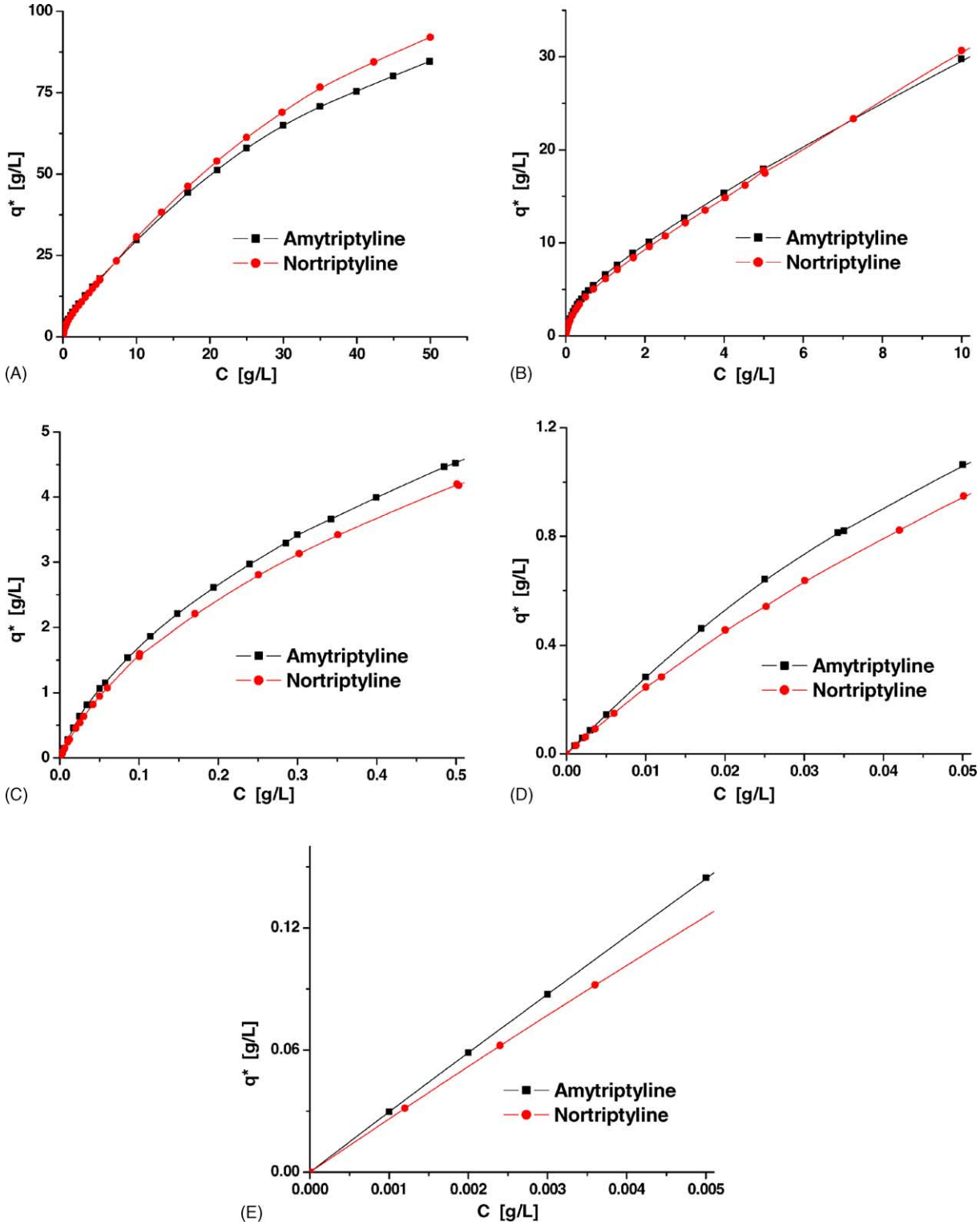

Fig. 1. Comparison between the single-component isotherms of nortriptyline and amytriptyline. Mobile phase: acetonitrile:water (28/72, v/v). Phosphate buffer, 20 mM, pH 2.70. C_{18}-Discovery column, $T = 295$ K. Concentration range (A) 0–50 g/L, (B) 0–10 g/L, (C) 0–0.5 g/L, (D) 0–0.05 g/L, and (E) 0–0.005 g/L. Note that the two isotherms cross at a concentration around 7 g/L.

rium with a mobile phase of concentration C^* were calculated as follows:

$$q^* = \frac{(V - \epsilon V_C)C^*}{(1-\epsilon)V_C} \quad (1)$$

where q^* is the equilibrium concentration of the compound in the adsorbed phase, V the elution volume measured by applying the equivalent area method to the front (i.e., the adsorption profile) of the single component breakthrough curve, V_C the column tube volume (cross-section area × length) and ϵ is the total porosity of the column derived from the elution volume of a "non-retained" compound.

In the case of binary isotherm data, the equilibrium concentrations, q_1^* and q_2^*, of the two components in the adsorbed phase are given by

$$q_1^* = \frac{(V_1 - \epsilon V_C)C_1^* - (V_2 - V_1)(C_1^i - C_1^*)}{(1-\epsilon)V_C} \quad (2a)$$

$$q_2^* = \frac{(V_2 - \epsilon V_C)C_2^*}{(1-\epsilon)V_C} \quad (2b)$$

where $V_0 = \epsilon V_C$, V_1, V_2 and $(1-\epsilon)V_C$ are the column hold-up volume, the elution volumes of the first and second breakthrough fronts or shock layers, and the volume of adsorbent in the column, respectively; C_1^*, C_2^* and C_1^i are the feed concentrations of components 1 and 2 and the concentration of component 1 in the intermediate plateau, respectively. Accordingly, the single-component calibration curve of component 1 is necessary to measure C_1^i at the column outlet. Because we do not use the staircase method, we do not need to analyze the composition of the eluate at the intermediate plateau.

2.2. Models of isotherm

The adsorption data measured in this work were fitted to the following isotherm models, using the Marquardt algorithm [18] which minimizes the residual sum of the squares of the relative differences between the experimental data and those calculated with the model.

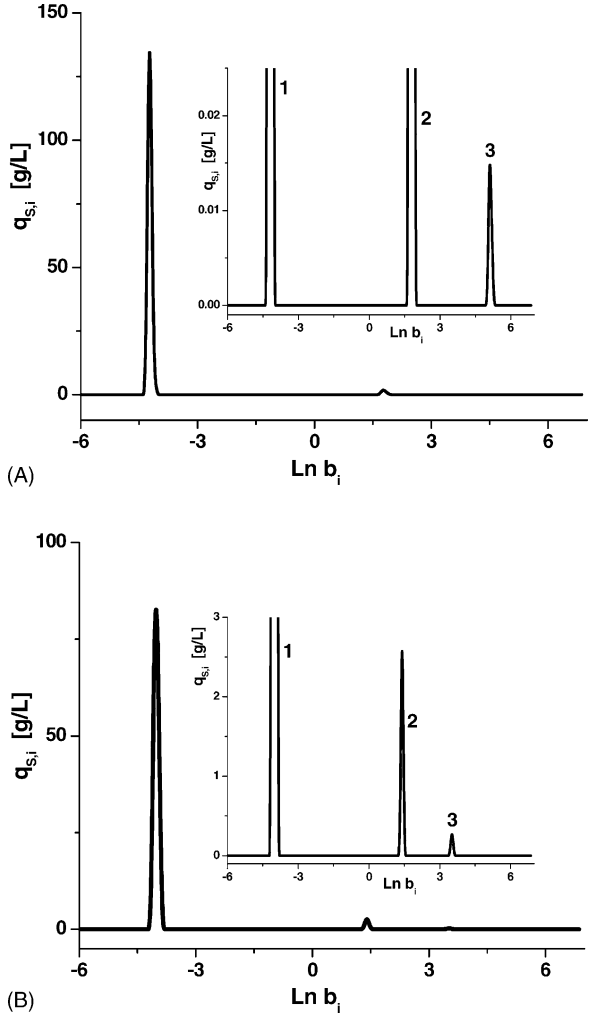

Fig. 2. Adsorption energy distributions (AEDs) of nortriptyline (A) and amytriptyline (B) calculated from the raw adsorption data shown in Fig. 1. The calculations were performed by using the expectation-maximization method, a local Langmuir isotherm and 100 millions iterations. Note the trimodal energy distribution for the two compounds.

2.2.1. Single component isotherm

The adsorption isotherm data of nortriptyline and amitriptylline on the C_{18}-Discovery column, from a mixture of acetonitrile and buffered water (28:72, v/v; 20 mM

Table 2
Comparison between the tri-Langmuir isotherm parameters accounted for by the adsorption of nortriptyline and amytriptyline (C_{18}-Discovery; acetonitrile–water; 28/72, v/v; 20 mM phosphate buffer; pH 2.70) obtained by MLRA of the single-component, two-component adsorption data and by the calculation of the AED

Compound (method)	Nortriptyline			Amytriptyline		
	MLRA 1 component	AED	MLRA[a] 2 components	MLRA 1 component	AED	MLRA[a] 2 components
$q_{s,1}$ (mmol/L)	771	712	651	578	544	651
b_1 (L/mmol)	0.0039	0.0043	0.0033	0.0051	0.0056	0.0052
$q_{s,2}$ (mmol/L)	11.3	11.2	14.5	11.1	12.3	14.5
b_2 (L/mmol)	1.20	1.78	0.76	0.68	0.44	0.75
$q_{s,3}$ (mmol/L)	1.5	0.10	2.2	4.5	1.29	2.2
b_3 (L/mmol)	6.84	49.4	6.09	4.46	10.6	7.33

[a] Fitting of the competitive adsorption data using the thermodynamically consistent model (Eqs. (6a) and (6b)).

phosphate; pH 2.70) are best described by a tri-Langmuir isotherm model, an extension of the classical Langmuir model to heterogeneous surfaces [13]. The tri-Langmuir isotherm model assumes a heterogeneous surface paved with three independent types of sites, each one consisting of homogeneous chemical domains that behave independently. The equilibrium isotherm results from the addition of three independent local Langmuir isotherms:

$$q^* = q_{s,1}\frac{b_1 C^*}{1+b_1 C^*} + q_{s,2}\frac{b_2 C^*}{1+b_2 C^*} + q_{s,3}\frac{b_3 C^*}{1+b_3 C^*} \quad (3a)$$

where $q_{s,1}$, $q_{s,2}$, $q_{s,3}$, b_1, b_2, b_3 are the monolayer saturation capacities and the low-concentration equilibrium constants on sites 1–3, respectively. The equilibrium constants b_1, b_2 and b_3 are associated with the adsorption energies $\epsilon_{a,1}$, $\epsilon_{a,2}$, and $\epsilon_{a,3}$, through the following equation [19]:

$$b_i = b_0 \mathrm{e}^{\frac{\epsilon_{a,i}}{RT}} \quad (3b)$$

where $\epsilon_{a,i}$ is the adsorption energy on sites i, R the universal ideal gas constant, and T is the absolute temperature and b_0 is a preexponential factor that could be derived from the molecular partition functions in both the bulk and the adsorbed phases. b_0 is often considered as independent of the adsorption energy $\epsilon_{a,i}$ [19]. Then the difference between the two adsorption energies associated with two different equilibrium constants, b_2 and b_1, is:

$$\epsilon_2 - \epsilon_1 = RT \ln\left(\frac{b_2}{b_1}\right) \quad (4)$$

2.2.2. Competitive binary isotherms

The binary competitive isotherm consistent with tri-Langmuir isotherm models for the two single-component isotherms can be written:

$$q_1^* = \frac{a_{1,1}C_1^*}{1+b_{1,1}C_1^*+b_{2,1}C_2^*} + \frac{a_{1,2}C_1^*}{1+b_{1,2}C_1^*+b_{2,2}C_2^*}$$

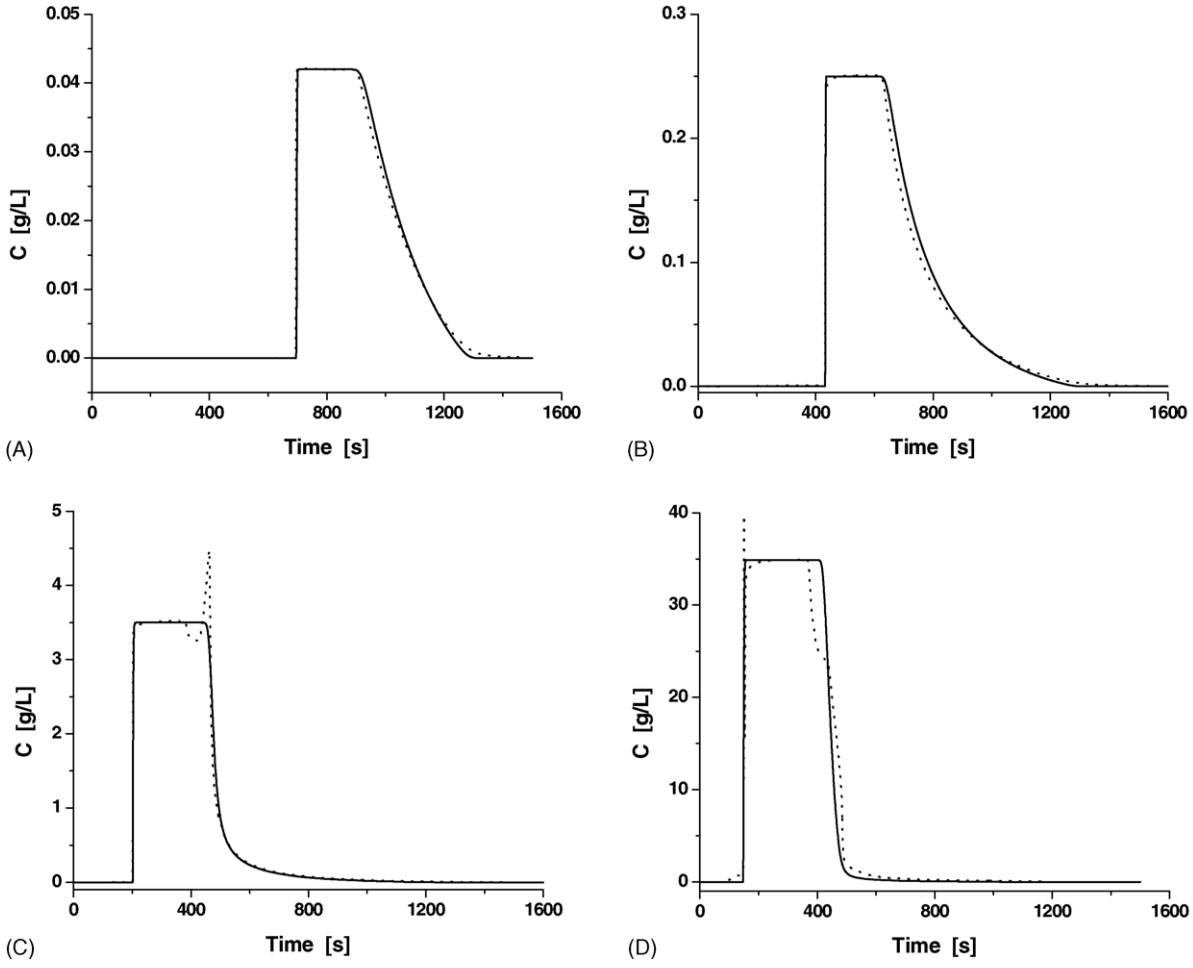

Fig. 3. Comparison between calculated (solid lines) and experimental (dotted lines) breakthrough curves of nortriptyline. The isotherm parameters used in the calculations are given in Table 2 (FA, 1 component). Same experimental conditions as in Fig. 1. (A) $C_{inj} = 0.04$ g/L, $t_{inj} = 360$ s; (B) $C_{inj} = 0.25$ g/L, $t_{inj} = 360$ s; (C) $C_{inj} = 3.5$ g/L, $t_{inj} = 300$ s; and (D) $C_{inj} = 35$ g/L, $t_{inj} = 300$ s.

$$+\frac{a_{1,3}C_1^*}{1+b_{1,3}C_1^*+b_{2,3}C_2^*} \quad (5a)$$

$$q_2^* = \frac{a_{2,1}C_2^*}{1+b_{1,1}C_1^*+b_{2,1}C_2^*} + \frac{a_{2,2}C_2^*}{1+b_{1,2}C_1^*+b_{2,2}C_2^*} + \frac{a_{2,3}C_2^*}{1+b_{1,3}C_1^*+b_{2,3}C_2^*} \quad (5b)$$

Thermodynamic consistency requires that the saturation capacities of the two compounds on each type of sites be the same. Otherwise, the competitive isotherm is thermodynamically inconsistent and, in practice, does not account well for the competitive behavior of the two compounds. The formulation in Eqs. (5a) and (5b) considers the Henry constants, $a_{i,j}$, of the component i on sites j. If, however, for a sake of consistency with the single component isotherm model (Eqs. (3a) and (3b)), we write a thermodynamically-consistent tri-Langmuir isotherm model with the same saturation capacities for the two components on each of the three types of sites, we have

$$q_1^* = q_{s,1}\frac{b_{1,1}C_1^*}{1+b_{1,1}C_1^*+b_{2,1}C_2^*} + q_{s,2}\frac{b_{1,2}C_1^*}{1+b_{1,2}C_1^*+b_{2,2}C_2^*} + q_{s,3}\frac{b_{1,3}C_1^*}{1+b_{1,3}C_1^*+b_{2,3}C_2^*} \quad (6a)$$

Table 3
Specific selectivities of each type of adsorption sites

Method	Selectivity (α-amytriptyline/nortriptyline)		
	MLRA 1 component	AED	MLRA[a] 2 components
Sites 1	0.98	1.00	1.58
Sites 2	0.56	0.27	0.99
Sites 3	1.96	2.77	1.20
Overall	1.14	0.79	1.14

Same experimental conditions as in Table 2.

[a] Fitting of the competitive adsorption data using the thermodynamically consistent model Eqs. (6a) and (6b)).

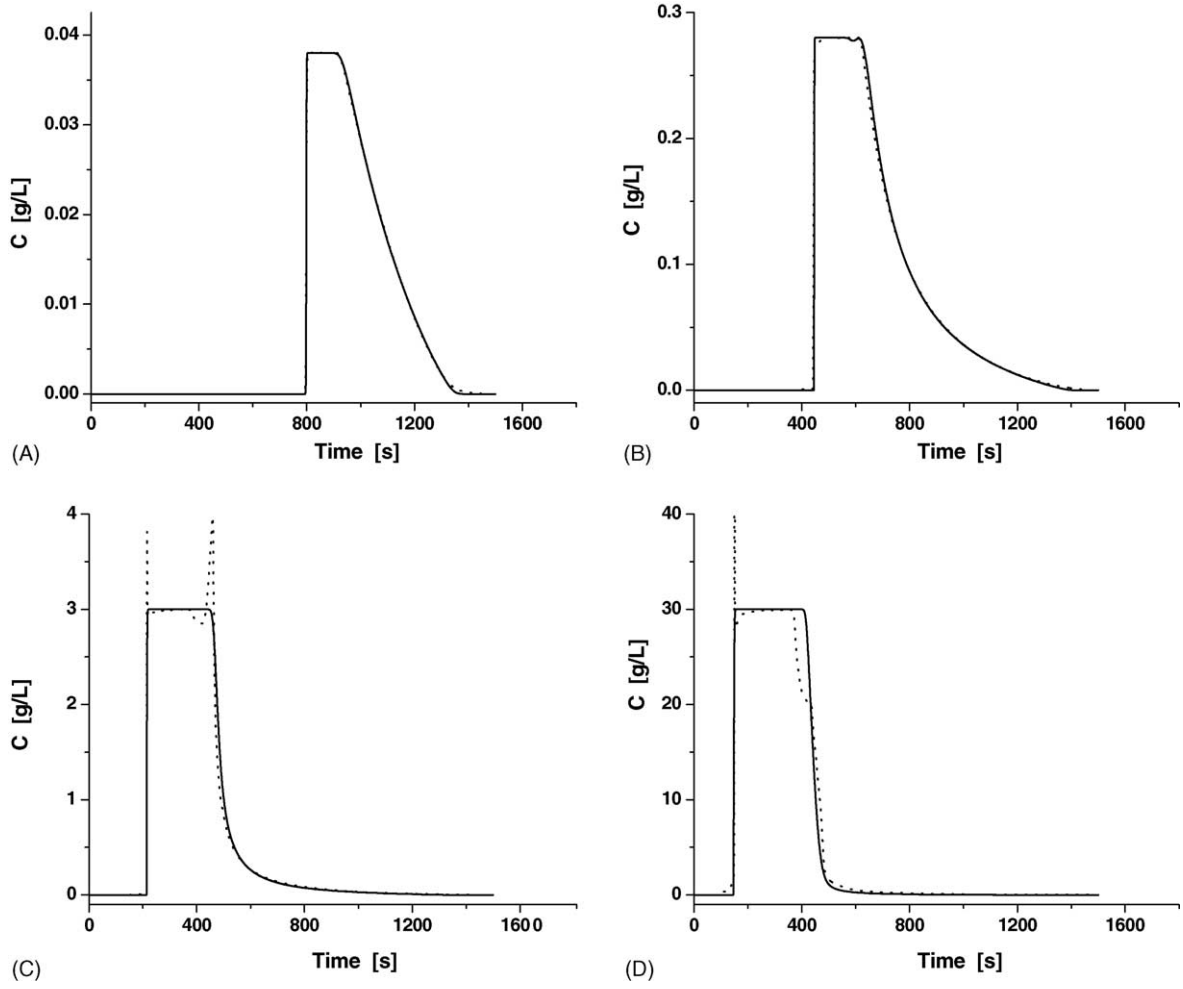

Fig. 4. Same as in Fig. 3 but for amytriptyline. (A) $C_{inj} = 0.038$ g/L, $t_{inj} = 300$ s; (B) $C_{inj} = 0.28$ g/L, $t_{inj} = 360$ s; (C) $C_{inj} = 3.0$ g/L, $t_{inj} = 300$ s; and (D) $C_{inj} = 35$ g/L, $t_{inj} = 300$ s.

$$q_2^* = q_{s,1}\frac{b_{2,1}C_2^*}{1+b_{1,1}C_1^*+b_{2,1}C_2^*} + q_{s,2}\frac{b_{2,2}C_2^*}{1+b_{1,2}C_1^*+b_{2,2}C_2^*} + q_{s,3}\frac{b_{2,3}C_2^*}{1+b_{1,3}C_1^*+b_{2,3}C_2^*} \quad (6b)$$

This model contains only nine independent parameters instead of the 12 parameters used in the former model. This is the consequence of the conditions imposed that $q_{s,1}$, $q_{s,2}$, and $q_{s,3}$ are the same for both compounds.

2.3. Calculation of the adsorption energy distributions

The calculation of the adsorption energy distribution (AED) was performed by using the expectation-maximization (EM) method [20]. The details of the algorithm applicable for any local isotherm (Langmuir, Jovanovic, Moreau or BET) are given in a previous publication [8].

2.4. Modeling of breakthrough curves and overloaded band profiles in HPLC

The breakthrough curves and the overloaded band profiles of nortriptyline, amytriptyline and their mixtures were calculated using the equilibrium-dispersive model (ED) of chromatography [1,21,22]. The ED model assumes instantaneous equilibrium between the mobile and the stationary phases and a finite column efficiency originating from an apparent axial dispersion coefficient, D_a, that accounts for axial dispersion and for all the mass-transfer resistances in the chromatographic column. This model describes successfully the overloaded band profiles of small or moderate molecular weight compounds in RPLC [23,24] when the mass transfer kinetics is fast enough and merely smooths the edges of the ideal band profiles predicted by thermodynamics alone.

In this study, the column efficiency was fixed at 5000 and 12,000 theoretical plates, depending on whether the compounds were injected from the HPLC pump or from the autosampler, respectively. The difference between these val-

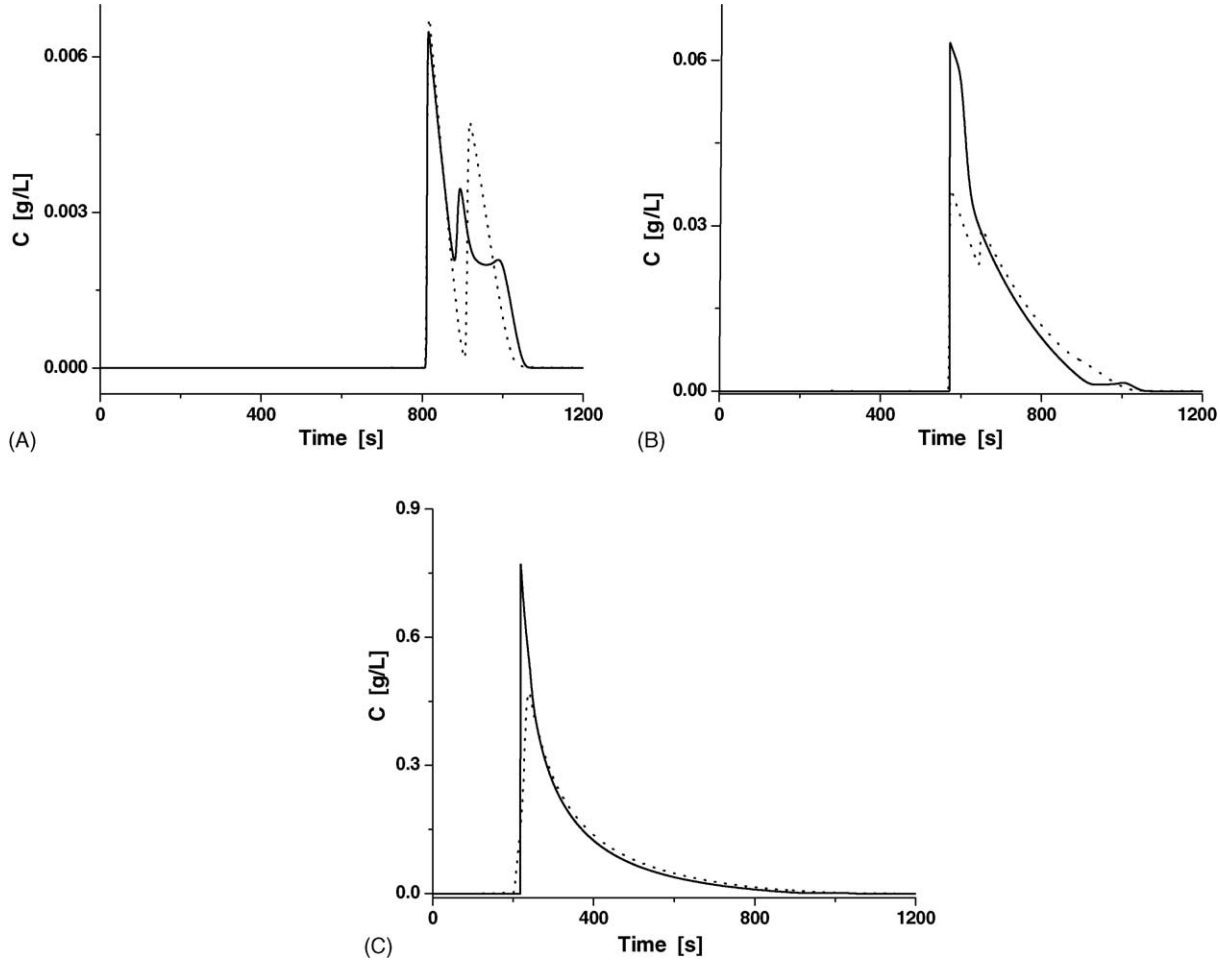

Fig. 5. Comparison between calculated (solid lines, competitive isotherms given by Eqs. (5a) and (5b)) and experimental (dotted lines) overloaded band profiles. Same experimental conditions as in Fig. 1. (A) $C_1 = 0.0427$ g/L, $C_2 = 0.0406$ g/L, $t_{inj} = 7.2$ s, (B) $C_1 = 0.1278$ g/L, $C_2 = 0.1271$ g/L, $t_{inj} = 7.2$ s, (C) $C_1 = 0.2377$ g/L, $C_2 = 0.2550$ g/L, $t_{inj} = 7.2$ s.

ues resides in a markedly lower contribution of axial dispersion in the extra-column volumes when the injection syringe is used. The extra-column volume is 0.035 ml with the syringe, 0.29 ml when the sample is delivered from the HPLC pump. Incidentally, this illustrates the importance of the injection mode used on the column efficiency actually achieved.

3. Experimental

3.1. Chemicals

The mobile phase used in this work was a mixture of acetonitrile and water (28:72, v/v), both HPLC grade, purchased from Fisher Scientific (Fair Lawn, NJ, USA). The solvents used to prepare the mobile phase were filtered before use on an SFCA filter membrane, 0.2 μm pore size (Suwannee, GA, USA). Thiourea was chosen to measure the column hold-up volume. Nortriptyline and amytriptyline hydrochloride were chosen as the two analytes in this work. These two compounds have the same large hydrophobic three-rings core, 10,11-dihydro-5H-dibenzo[a,d]cyclohepten-5-ylidene, and nearly the same amino spacer (*N*-methyl and *N*-dimethyl-1-propanamine, respectively). They differ by the presence of an additional methyl group in the spacer. Thiourea, nortriptyline and amytriptyline hydrochloride were all obtained from Aldrich (Milwaukee, WI, USA). Phosphoric acid (85%, w/w) and potassium dihydrogenophophate, used to prepare the buffer solutions at pH 2.70, were also purchased from Aldrich. The buffer pH was fixed at 2.70 (before the addition of the organic modifier) by mixing the buffer acidic solution (1368 μL H_3PO_4 85% in a 1 L volumetric glass) with the buffer basic solution (2.722 g in a 1 L volumetric glass), in the correct proportion (30.5/69.5, v/v).

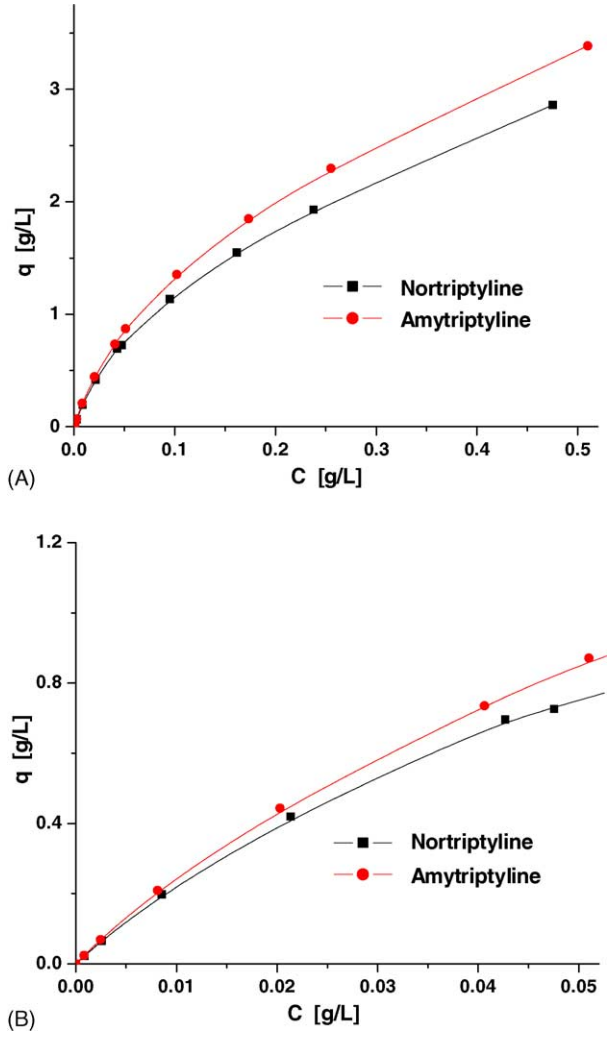

Fig. 6. Competitive adsorption data of nortriptyline and amytriptyline measured by FA. Same experimental conditions as in Fig. 1. Concentration range (A) 0–0.5 g/L and (B) 0–0.05 g/L.

3.2. Columns

The column used in this work was a 150 mm × 4.0 mm Discovery-C_{18} column from Supelco (Supelco Park, Bellefonte, PA, USA). The main characteristics of the bare porous silica and of the packing material used are summarized in Table 1. The hold-up volume of this column was measured by three independent methods; (1) the elution of a supposedly "unretained" compound (thiourea); (2) the minor disturbance method; and (3) the pycnometry measurements [13]. The values obtained with these three methods were, respectively, 1.363, 1.378, and 1.349 mL. In all the calculations (adsorption data, calculation of the band profiles), the volume measured by injecting thiourea was used (1.363 mL). The total porosity of the column is then $\epsilon = 0.7231$.

3.3. Apparatus

The isotherm data were acquired using a Hewlett-Packard (Palo Alto, CA, USA) HP 1090 liquid chromatograph. This instrument includes a multi-solvent delivery system (tank volumes, 1 L each), an auto-sampler with a 25 μL sample loop, a diode-array UV-detector, a column thermostat and a data station. Compressed nitrogen and helium bottles (National Welders, Charlotte, NC, USA) are connected to the instrument to allow the continuous operations of the pump, the auto-sampler, and the solvent sparging. The extra-column volumes are 0.035 and 0.29 mL as measured from the auto-sampler and from the pump system, respectively, to the column inlet. All the retention data were corrected for these contributions. The flow-rate accuracy was controlled by pumping the pure mobile phase at 23 °C and 1 mL/min during 50 min, from each pump head, successively, into a volumetric glass of 50 mL. The relative error was less than 0.4%, so that we can estimate the long-term accuracy of the flow-rate at 4 μL/min at flow rates around 1 mL/min. All measurements were carried out at a constant tempera-

ture of 21 °C, fixed by the laboratory air-conditioner. The daily variation of the ambient temperature never exceeded ±1 °C.

3.4. Measurements of the single and competitive adsorption isotherms by FA

The solubility of nortryptiline and amytriptyline largely exceed 100 g/L in a acetonitrile:water solutions of any composition between 15:85 and 30:70 (v/v). The maximum concentration used in the FA measurements for single-component isotherms was fixed at 50 g/L. The minimum concentration was adjusted by trial and error, so as to make sure that the adsorption isotherm behaved linearly. Successive master solutions of nortryptiline and amytriptyline were prepared at 50, 5, 0.5, and 0.05 g/L. The UV-detector detection limits was reached when 2% of the last solution was mixed to the pure mobile phase ($\lambda_{max} = 208$ nm, C = 0.001 g/L, or ≤ 3.5 μmol). Consecutive FA runs were then performed starting from the highest to the lowest concentrations, until the linear regime was reached (e.g. symmetrical breakthrough curves were recorded). For each FA run, pump A of the HPLC instrument was used to deliver a stream of pure mobile phase (acetonitrile:water, 28:72, v/v; non-buffered or buffered at pH 2.70) while pump B delivers a stream of the mother solution. The concentration of the compounds in the FA stream is determined by the concentration of the mother sample solution and the flow rate fractions delivered by the two pumps. Because mixing is performed under atmospheric pressure, no corrections are needed for the mixing volume. The breakthrough curves were all recorded at a flow rate of 1 mL min^{-1}, with a sufficiently long time delay between successive breakthrough curve to allow for complete reequilibration of the column with the pure mobile phase. The injection time of the sample was between 5 and 6 min, in order to reach a stable plateau at the column outlet. The signal was recorded at 299, 290, 255, and 220 nm with the master solutions at concentrations of 50, 5, 0.5, and 0.05 g/L, respectively. For each wavelength, a calibration curve was measured from the UV detected signal at the equilibrium plateau and was used to

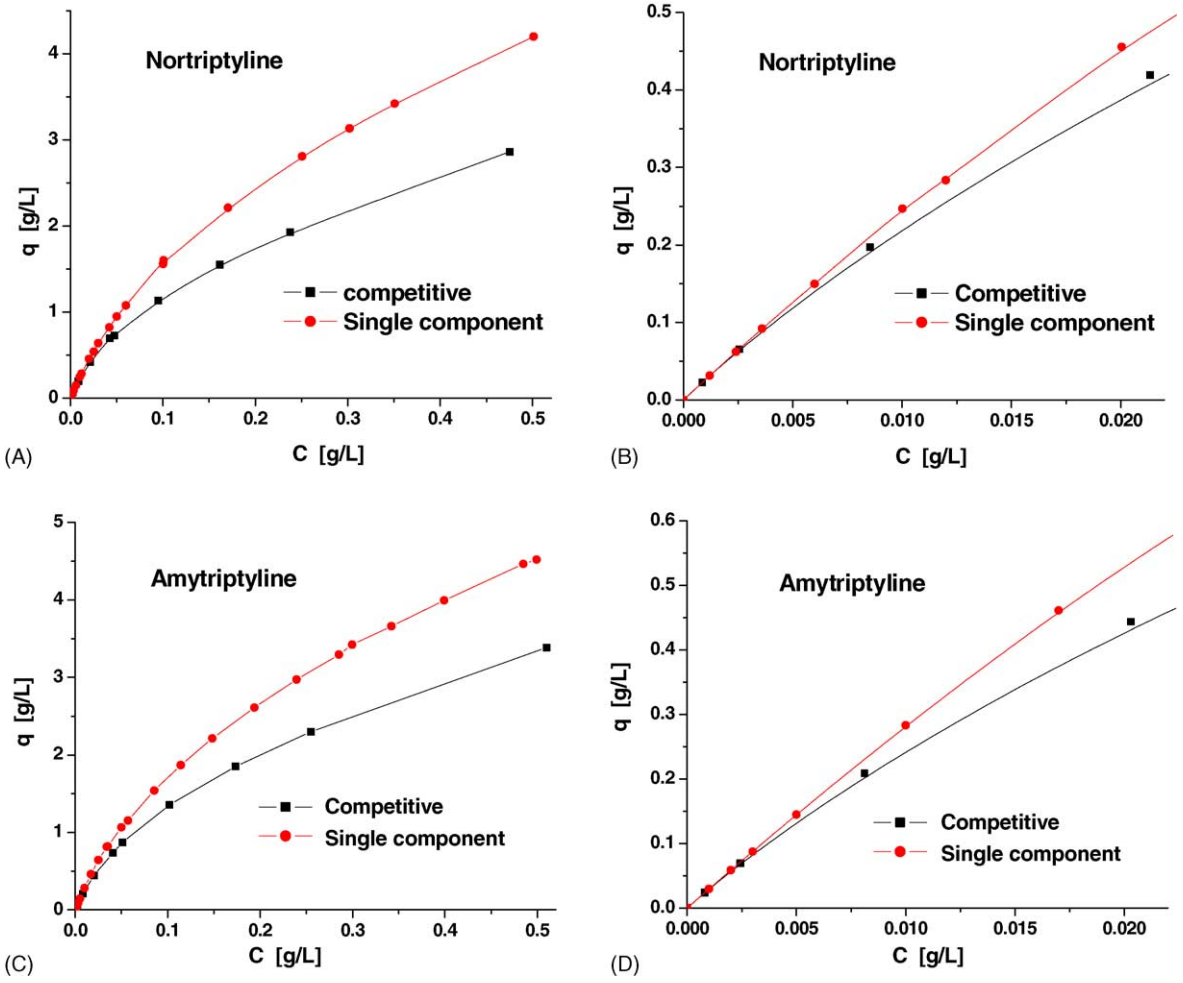

Fig. 7. Comparison between the two-component competitive and the single-component adsorption data. Same experimental conditions as in Fig. 1. (A) Nortriptyline, concentration range 0–0.5 g/L; (B) nortriptyline, 0–0.02 g/L; (C) amytriptyline, concentration 0–0.5 g/L; and (D) amytriptyline 0–0.02 g/L.

transform the absorbance signal (mAU) into concentration (g/L) for all the band profiles recorded.

The competitive adsorption data were measured by pumping solutions of nortriptyline and amytriptyline hydrochloride at the same concentration in g/L ($C_1 = C_2$). This concentration ratio is the one that maximizes the competition for adsorption onto the surface between the two compounds [16]. Three master solutions at 0.05, 0.5, and 5 g/L were prepared before recording the competitive breakthrough curves at 220, 255, and 275 nm, respectively. Calibration curves were

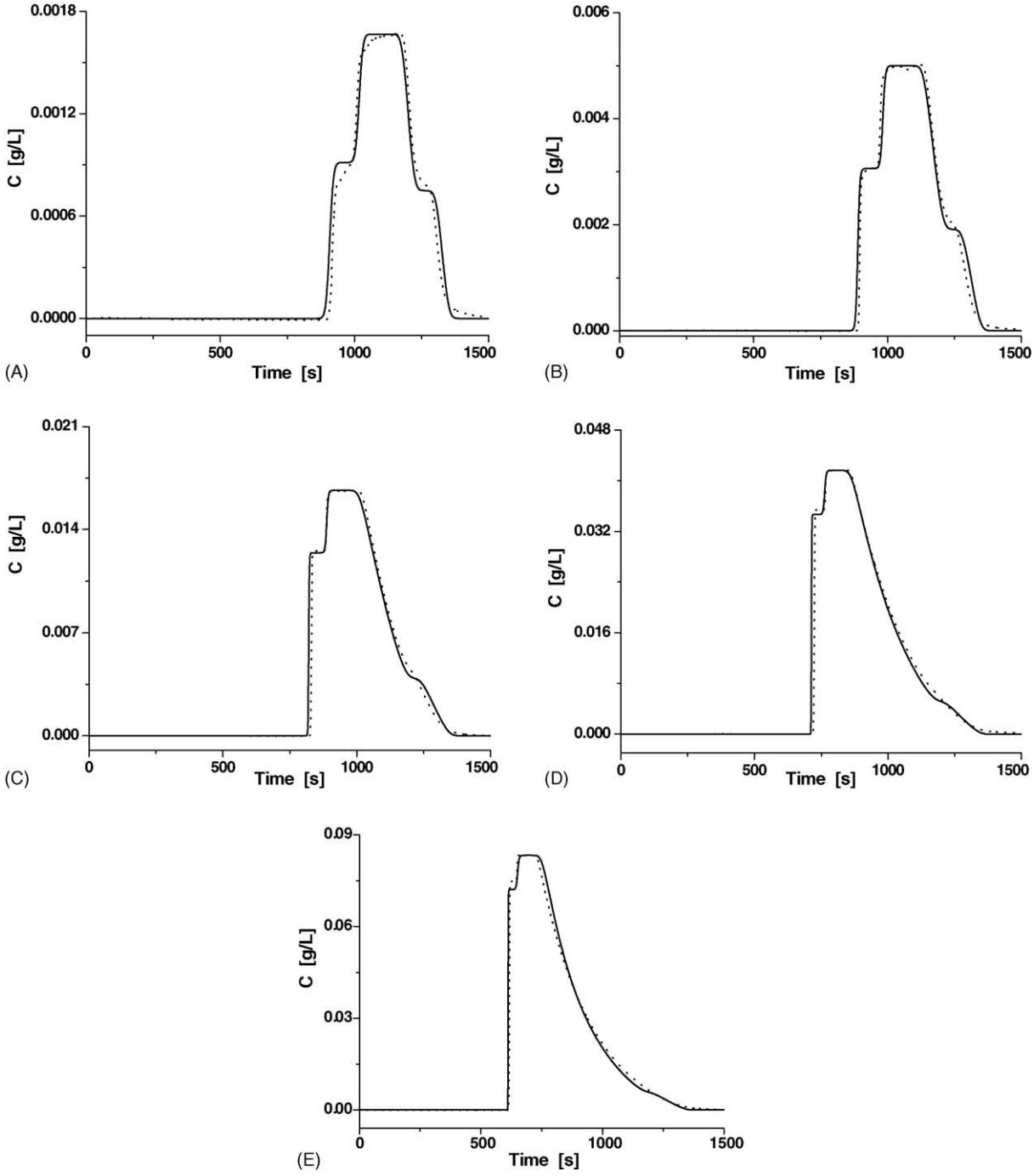

Fig. 8. Comparison between the simulated (solid lines, competitive isotherms given by Eqs. (6a) and (6b)) and experimental (dotted lines) two-component breakthrough curves of nortriptyline (component 1) and amytriptyline (component 2). Same experimental conditions as in Fig. 1. (A) $C_1 = 0.000854$ g/L, $C_2 = 0.000812$ g/L $t_{inj} = 300$ s; (B) $C_1 = 0.002562$ g/L, $C_2 = 0.002436$ g/L $t_{inj} = 300$ s; (C) $C_1 = 0.00854$ g/L, $C_2 = 0.00812$ g/L $t_{inj} = 300$ s; (D) $C_1 = 0.02135$ g/L, $C_2 = 0.0203$ g/L $t_{inj} = 300$ s; (E) $C_1 = 0.0427$ g/L, $C_2 = 0.0406$ g/L $t_{inj} = 300$ s; (F) $C_1 = 0.09508$ g/L, $C_2 = 0.1022$ g/L $t_{inj} = 300$ s; (G) $C_1 = 0.1616$ g/L, $C_2 = 0.1737$ g/L $t_{inj} = 300$ s; (H) $C_1 = 0.2377$ g/L, $C_2 = 0.255$ g/L $t_{inj} = 300$ s; and (I) $C_1 = 0.4754$ g/L, $C_2 = 0.511$ g/L $t_{inj} = 300$ s.

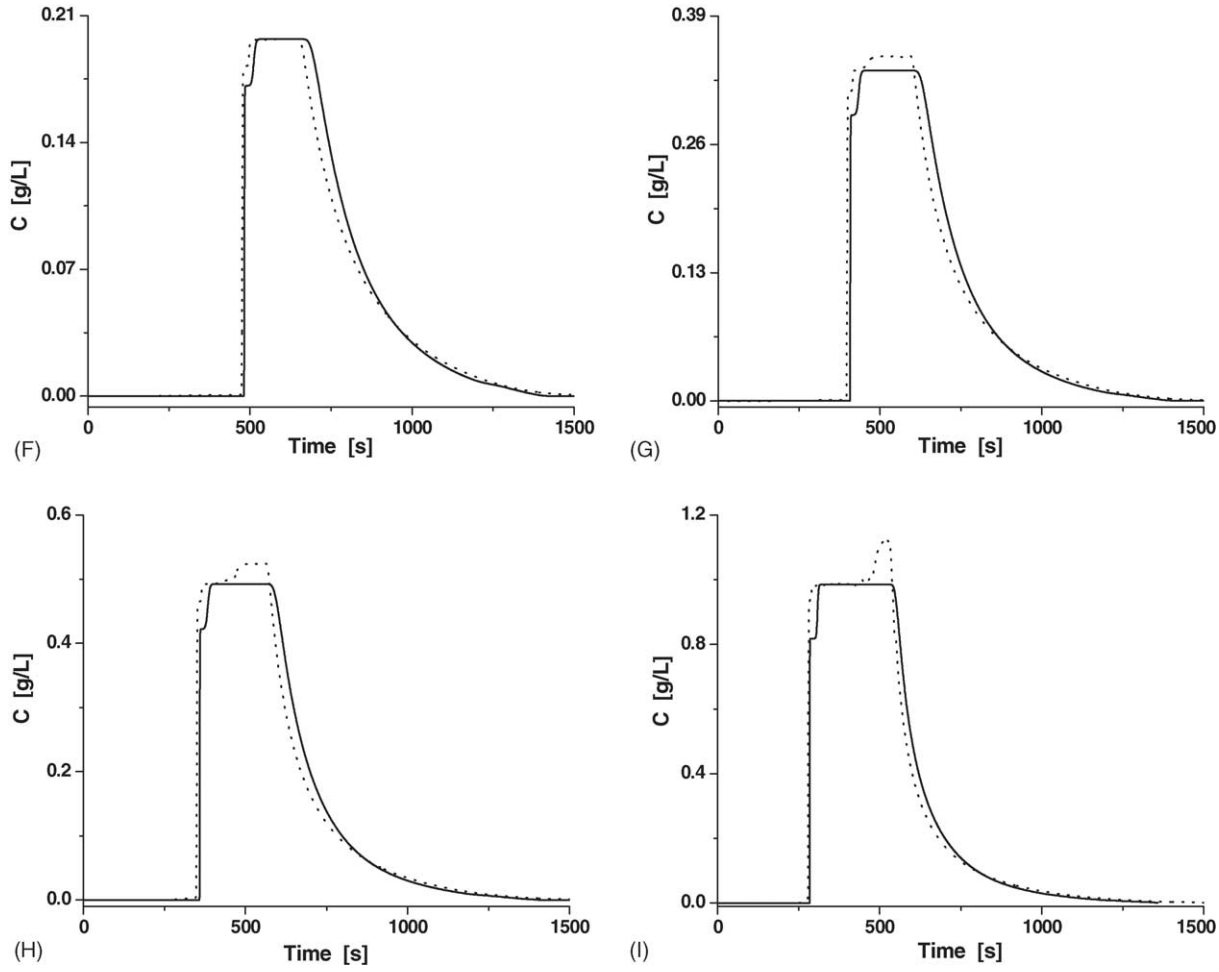

Fig. 8. (*Continued*).

measured for each wavelength at the equilibrium plateau, $C_1 + C_2 = f(\mathrm{mAU}_1 + \mathrm{mAU}_2)$. Since both compounds have the same absorbance at these wavelengths, $C_1 = f(\mathrm{mAU}_1)$, $C_2 = f(\mathrm{mAU}_2)$ and the total UV absorbance signal was directly recalculated with the same calibration curve *f*.

4. Results and discussion

4.1. Single component isotherms

The adsorption isotherms of nortriptyline and amytriptyline are shown in Fig. 1A–E. The best isotherm model accounting for these data is the tri-Langmuir isotherm model. For both compounds, the calculations of the AED converged toward a trimodal distribution, confirming the choice of the heterogeneous adsorption isotherm model (Fig. 2A and B). The best parameters of the tri-Langmuir isotherm and the specific selectivities for both compounds on the three different types of sites are listed in Tables 2 and 3, respectively. Significant discrepancies are observed between the parameters derived from the EM program and those derived from the MLRA method. The EM program uses the raw adsorption data measured by FA and should give results consistent with those derived from the isotherm modeling of these FA data. Previous use of this program has so far given results consistent with the parameters derived by MRLA, except that the agreement becomes poor for the types of sites that have a low saturation capacity, typically one smaller than 1 mmol/L. This confirms that both methods are very sensitive to the precision of the adsorption data acquired [25]. However, the two methods are consistent regarding the degree of heterogeneity measured and the order of magnitude of all the parameters.

Three types of adsorption sites account for the adsorption of nortriptyline and amytriptyline. The sites of lowest energy correspond to the adsorption of the analytes at the interface of the C_{18}-bonded layer and the solution. These sites are the most numerous, accounting for at least 95% of the total saturation capacity. The sites of intermediate energy represent about 2% of the total column capacity and correspond most probably to adsorption sites located inside the hydrocarbon layer. For the sake of comparison, the sites of this type account for about 30 and 6% of the total column saturation capacity of

six commercial brands of RPLC phases for phenol (one ring, molar mass, ca. 100 g/mol) and caffeine (two rings, molar mass, ca. 200 g/mol), respectively [11]. The fact that the sites of intermediate energy account for only 2% of the column saturation capacity is certainly explained by the larger size of the molecules of nortriptyline and amytriptyline, which have three hydrocarbon rings (two phenyl, one cycloheptene) and a molecular mass around 300 g/mol. The larger the analyte molecule, the fewer the cavities in the bonded layer that it can access and the lower the corresponding saturation capacity. Finally there is a significant number of high energy sites that are located deep inside the C_{18} layer, where analyte molecules may simultaneously interact with the bonded alkyl chains and the silica support, i.e. with isolated silanol groups that might not have been endcapped or with siloxane bridges. These sites account for less than 0.5% of the total saturation capacity. Obviously, there are no possible ionic interactions between these ionizable compounds (nortriptyline and amytriptyline are positively charged at pH 2.70) and ionized silanols because the pH is too acidic (the retention factor of a small cation like Li^+ or a larger one like bretylium ([*o*-bromo-benzyl]ethyldimethyl ammonium) on endcapped C_{18}-bonded phases is zero for pH's below 6 [26,27]).

Figs. 3A–D and 4A–D compare the profiles of experimental breakthrough curves and of curves calculated on the basis of the single-component isotherm parameters given in Table 2. A column efficiency of 5000 was assumed in all calculations. The agreement is excellent with all plateau concentrations between 0 and 50 g/L. The isotherm parameters obtained by multi-linear regression analysis (MLRA) of the adsorption data are validated because the diffuse rear boundary of the experimental breakthrough curves, a boundary that is not involved in the derivation of the adsorption isotherm data, matches almost perfectly that of the calculated curves. Some minor deviations are observed for concentrations larger than a few grams per liter. Such anomalies of the rear part of

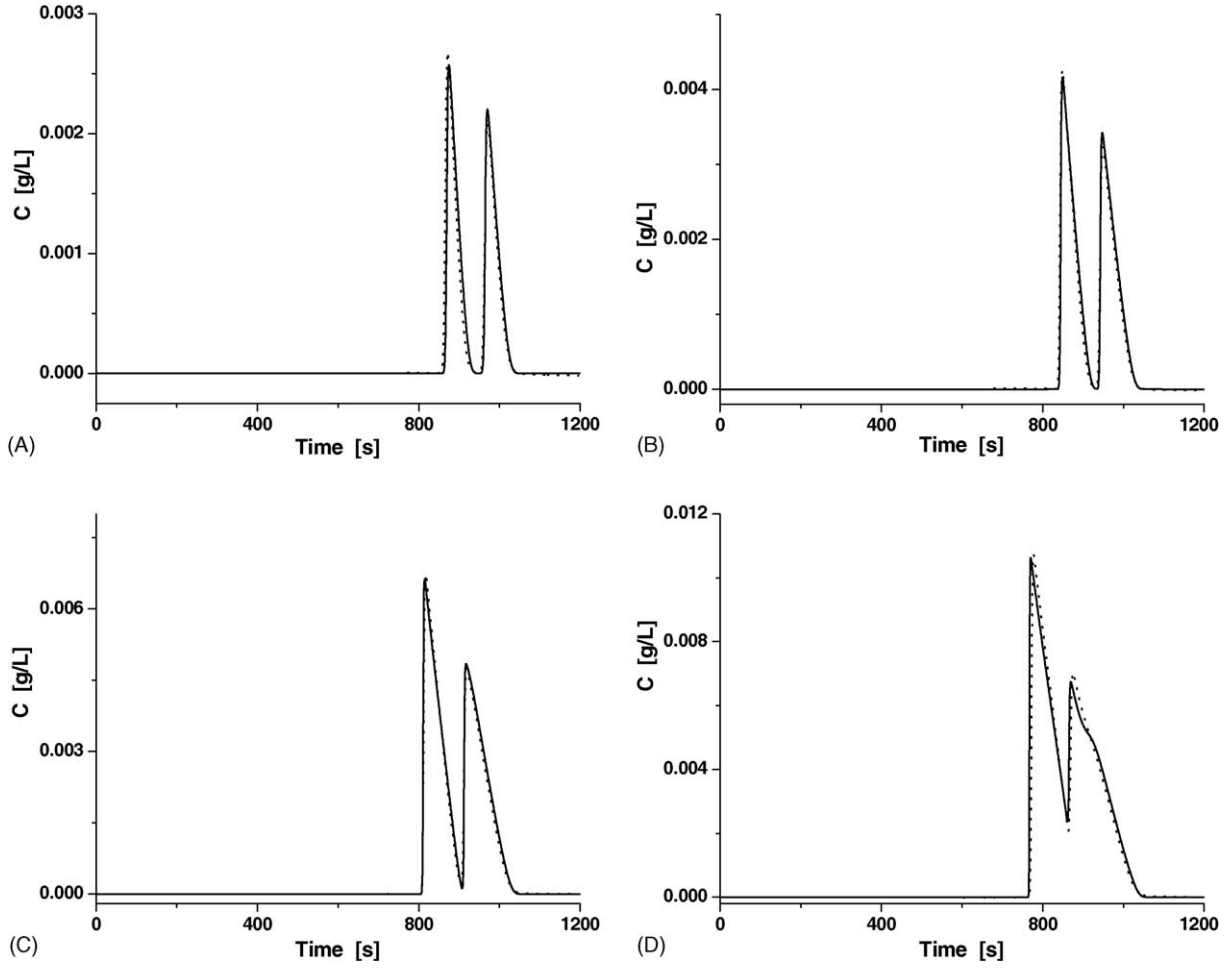

Fig. 9. Comparison between the simulated (solid lines, competitive isotherms given by Eqs. Eqs. (6a) and (6b)) and experimental (dotted lines) two-component overloaded band profiles of nortriptyline (component 1) and amytriptyline (component 2). Same experimental conditions as in Fig. 1. (A) $C_1 = 0.0427$ g/L, $C_2 = 0.0406$ g/L $t_{inj} = 1.8$ s; (B) $C_1 = 0.0427$ g/L, $C_2 = 0.0406$ g/L $t_{inj} = 3.6$ s; (C) $C_1 = 0.0427$ g/L, $C_2 = 0.0406$ g/L $t_{inj} = 7.2$ s; (D) $C_1 = 0.0427$ g/L, $C_2 = 0.0406$ g/L $t_{inj} = 14.4$ s; (E) $C_1 = 0.4754$ g/L, $C_2 = 0.511$ g/L $t_{inj} = 1.8$ s; (F) $C_1 = 0.4754$ g/L, $C_2 = 0.511$ g/L $t_{inj} = 3.6$ s; (G) $C_1 = 0.4754$ g/L, $C_2 = 0.511$ g/L $t_{inj} = 7.2$ s; (H) $C_1 = 0.4754$ g/L, $C_2 = 0.511$ g/L $t_{inj} = 14.4$ s; (I) $C_1 = 5.112$ g/L, $C_2 = 5.084$ g/L $t_{inj} = 1.8$ s; (J) $C_1 = 5.112$ g/L, $C_2 = 5.084$ g/L $t_{inj} = 3.6$ s; (K) $C_1 = 5.112$ g/L, $C_2 = 5.084$ g/L $t_{inj} = 7.2$ s; and (L) $C_1 = 5.112$ g/L, $C_2 = 5.084$ g/L $t_{inj} = 14.4$ s.

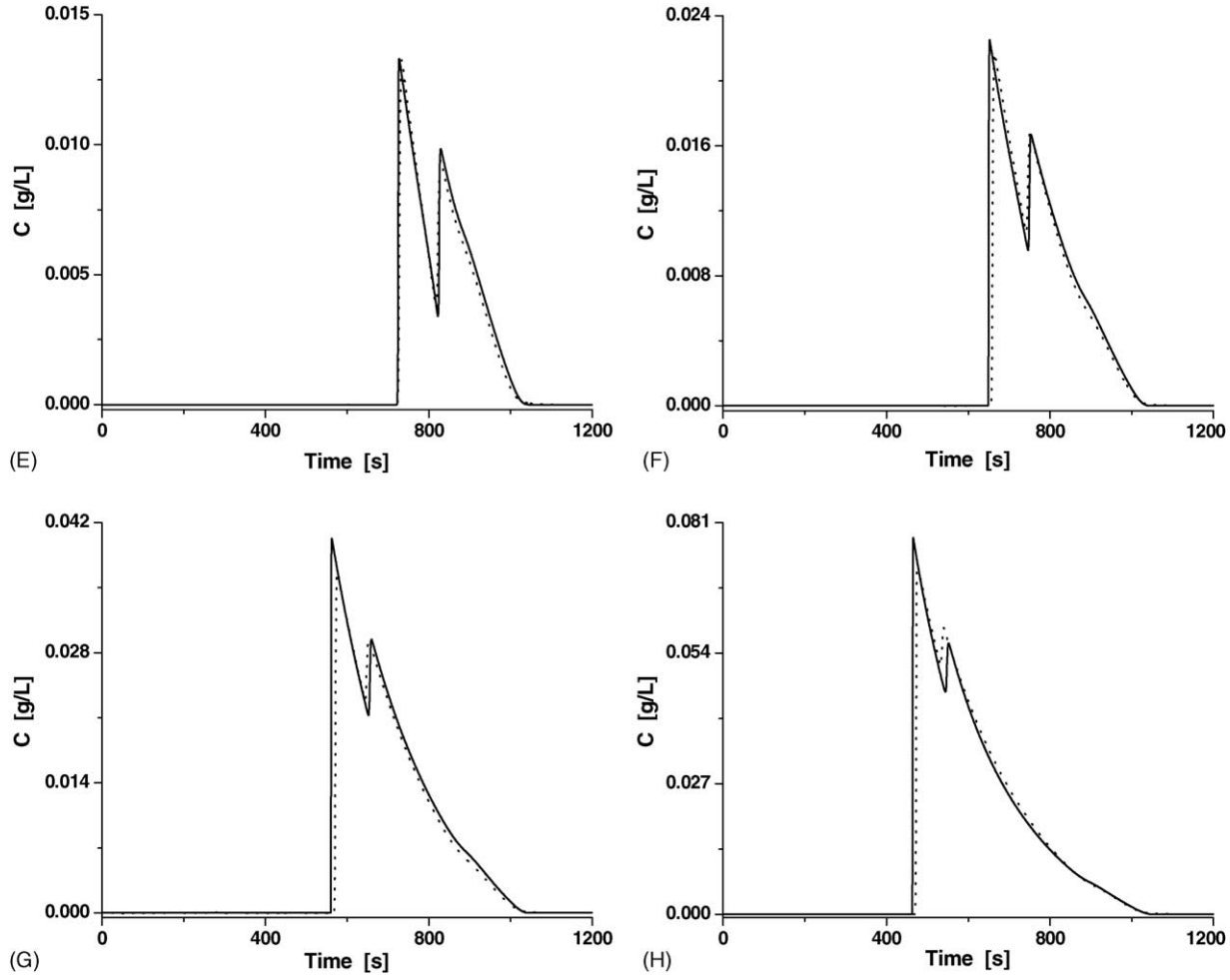

Fig. 9. (*Continued*)

the band profiles could be explained by the complex solute mass transfer that takes place through the acetonitrile multilayer adsorbed phase (there are about four molecular layers of acetonitrile adsorbed in the alkyl bonded layer). These anomalies do not occur when methanol is used as the organic mobile phase modifier because methanol adsorbs as a mere monolayer on the C_{18}-bonded surface.

4.2. Competitive adsorption isotherm

The validated single-component tri-Langmuir isotherms were used to build up a two-component competitive isotherm model, using Eqs. (5a) and (5b). In these equations, the terms $a_{i,j} = q_{S,i,j}b_{i,j}$ are directly calculated from the products of the saturation capacity and the equilibrium constant for each component i, on each site j. Obviously, the model thus obtained is thermodynamically inconsistent. Nevertheless, such a model was successfully applied earlier to the calculation of the band profiles of mixtures of C_{60} and C_{70}, in which case the single-component isotherms were bi-Langmuir isotherms [28]. However, this simple approach does not apply here. Fig. 5A–C compare the overloaded band profiles (dashed lines) recorded for 100 μL samples of mixtures of nortriptyline and amytriptyline (concentrations 0.05, 0.5, and 5 g/L, respectively, and those calculated from this isotherm model (solid lines). For each set of profiles there are important discrepancies. In Fig. 5A, the band of the most retained compound, amytriptyline, is definitely incorrect. In Fig. 5B and C, the model predicts a reversal of the elution order of the two compounds (amytriptyline should elute first at high concentrations while it elutes last at low concentrations). Although this reversal is consistent with a tri-Langmuir isotherm model because it is a reflection of the different concentration dependencies of the three contributions (see Fig. 1A and B), this situation does not match the experimental data. Hence, a different approach is needed to obtain a more satisfactory competitive isotherm model. A set of competitive adsorption data needs to be acquired that involves the effects of the actual competition.

Competitive breakthrough curves were recorded for concentrations between 0 and 0.5 g/L of each component (equal concentrations of nortriptyline and amytriptyline). No useful data could be obtained for higher concentrations, however, because the breakthrough fronts of the two components

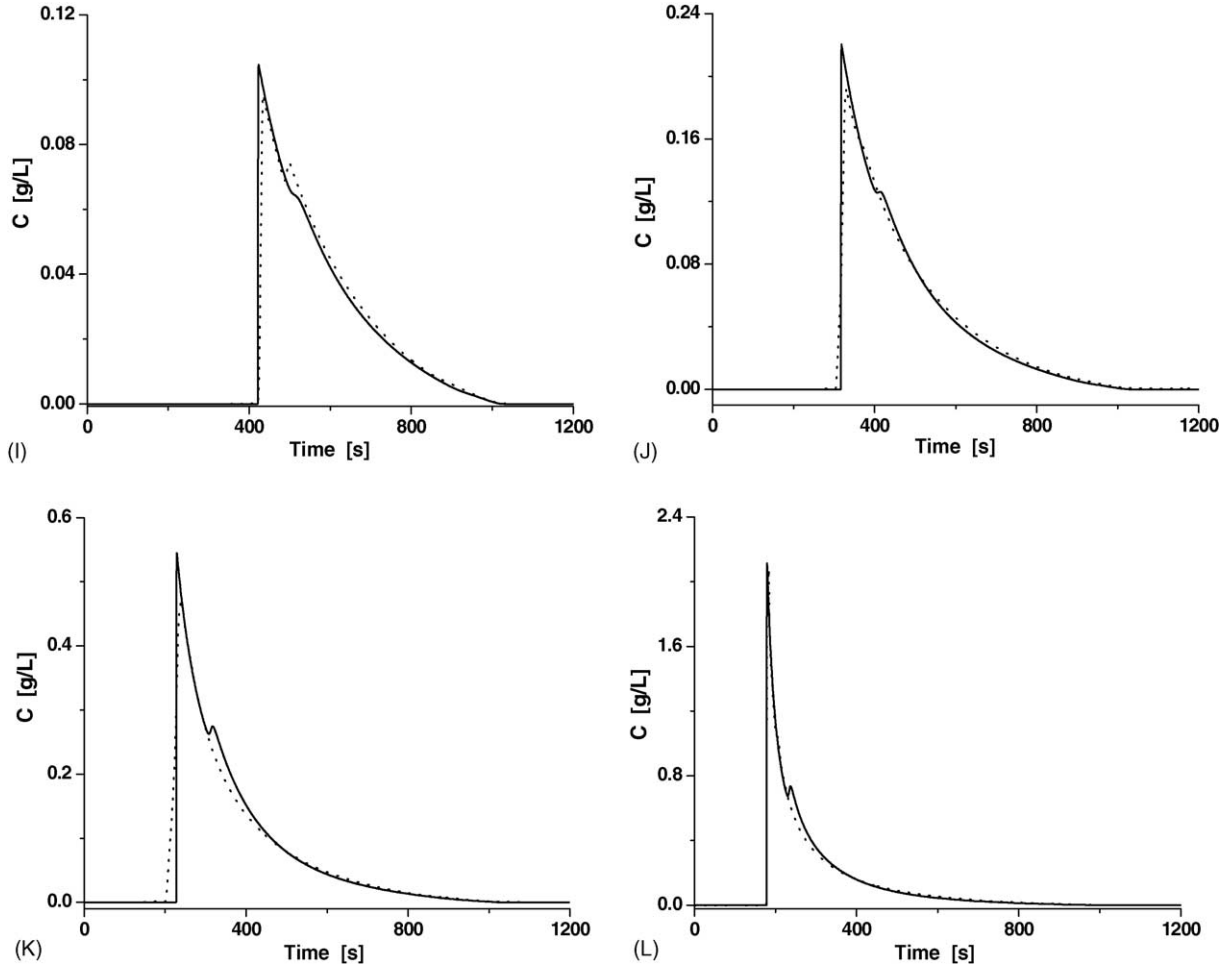

Fig. 9. (*Continued*).

could no longer be distinguished, making the measurements of the adsorption data of each compound both inaccurate and imprecise. Eqs. (2a) and (2b)) were used to calculate the amounts adsorbed, q_1^* and q_2^*. The competitive adsorption data are shown in Fig. 6A and B, in the range from 0.001 to 0.5 g/L. Fig. 7 compares the amounts adsorbed at equal mobile phase concentration of either compound, from its single-component and from the two-component solutions. This figure clearly confirms that competition for adsorption takes place in this system, even at very low concentrations. The single-component and the two-component isotherms of each compound are clearly distinct above a mobile phase concentration of, ca. 0.003 g/L. Note also that, up to 0.5 g/L, there is no reversal of the adsorption order of amytriptyline and nortriptyline. This reversal is expected only at higher concentrations, ca. 7 g/L (Fig. 1B). No specific adsorbate–adsorbate interactions seem to take place in the stationary phase. The sets of adsorption data $q_{1,\mathrm{exp}}$ and $q_{2,\mathrm{exp}}$ were simultaneously fitted to the competitive isotherm model ($q_1(C_1, C_2)$, $q_2(C_1, C_2)$) given in Eqs. (6a) and (6b). The nine parameters, $q_{S,1}$, $q_{S,2}$, $q_{S,3}$, $b_{1,1}$, $b_{2,1}$, $b_{1,2}$, $b_{2,2}$, $b_{1,3}$ and $b_{2,3}$, were adjusted by minimizing the sum of residual squares, using the solver option tool of Excel (Microsoft, Redmont, WA, USA):

$$\mathrm{Min}\sum_i \left(\frac{q^i_{1,\mathrm{exp}} - q_1(C^i_1, C^i_2)}{q^i_{1,\mathrm{exp}}}\right)^2 + \left(\frac{q^i_{2,\mathrm{exp}} - q_2(C^i_1, C^i_2)}{q^i_{2,\mathrm{exp}}}\right)^2$$

The best values obtained for the isotherm parameters are given in Table 2. It is noteworthy that the values of all these parameters are close to those derived from the single-component data. They are also in reasonably good agreement with the parameters derived from the AEDs of the individual components, in spite of significant differences. The validity of the set of numerical parameters of the empirical competitive isotherm obtained is demonstrated in Figs. 8A–I (which compares experimental and calculated breakthrough curves) and Fig. 9. (which compares experimental and calculated overloaded elution band profiles). The agreement between the corresponding profiles is now excellent in all cases, for both components simultaneously. Even relatively minor details of the profiles (e.g., the position and the height of the intermediate plateaus of the breakthrough curves, the position and height of the maximums of the two elution bands and of the valley in

between) are in close agreement. This detailed agreement between the profiles shows that competition is well accounted for by the competitive isotherm model. The only significant deviations observed take place on the top of the concentration plateaus of the breakthrough curves, at concentrations higher than 0.5 g/L (Fig. 8H and I). FA is not a very accurate method to measure competitive adsorption data under such conditions that the front shocks of the two compounds elute to closely and the intermediate plateau vanishes. This limitation is paid for by a relatively poor agreement between the fronts of the experimental and the calculated breakthrough curves. These spurious peaks and nicks at the edge of high concentration plateaus take place systematically with acetonitrile but never with methanol. This phenomenon is related to the cooperative adsorption of acetonitrile and the solutes. It will be discussed elsewhere [29].

Note that the single-component breakthrough curves already recorded are also in close agreement with those calculated using the new set of parameters, as illustrated in Figs. 10A–D and 11A–D. Due to the large number of parameters in the model, there is a degree of compensation between the three Langmuir contributions and the optimum values of the nine parameters that are not as sharply defined as they are with models having fewer parameters. This illustrates a general problem encountered in the determination of multicomponent isotherms. Single-component data are far easier to determine than multicomponent data, yet the multicomponent isotherms derived from a limited set of multicomponent isotherm data are far more accurate than those derived from single-component data. So, the isotherm parameters derived from competitive adsorption data should always be preferred to those determined from single-component adsorption data because they contain more experimental information on the system and predict correctly the overloaded band profiles of mixtures.

The isotherm contributions of the three types of sites exhibit quite different characteristics and the study of these differences gives useful clues regarding the retention mechanism. The saturation capacities of the types of sites 1–3 are in the proportion of 300, 20, and 1, respectively. These figures are similar to those found for other similar stationary phases, Kromasil-C_{18}, Symmetry-C_{18}, Xterra- C_{18}, Luna-C_{18}. From

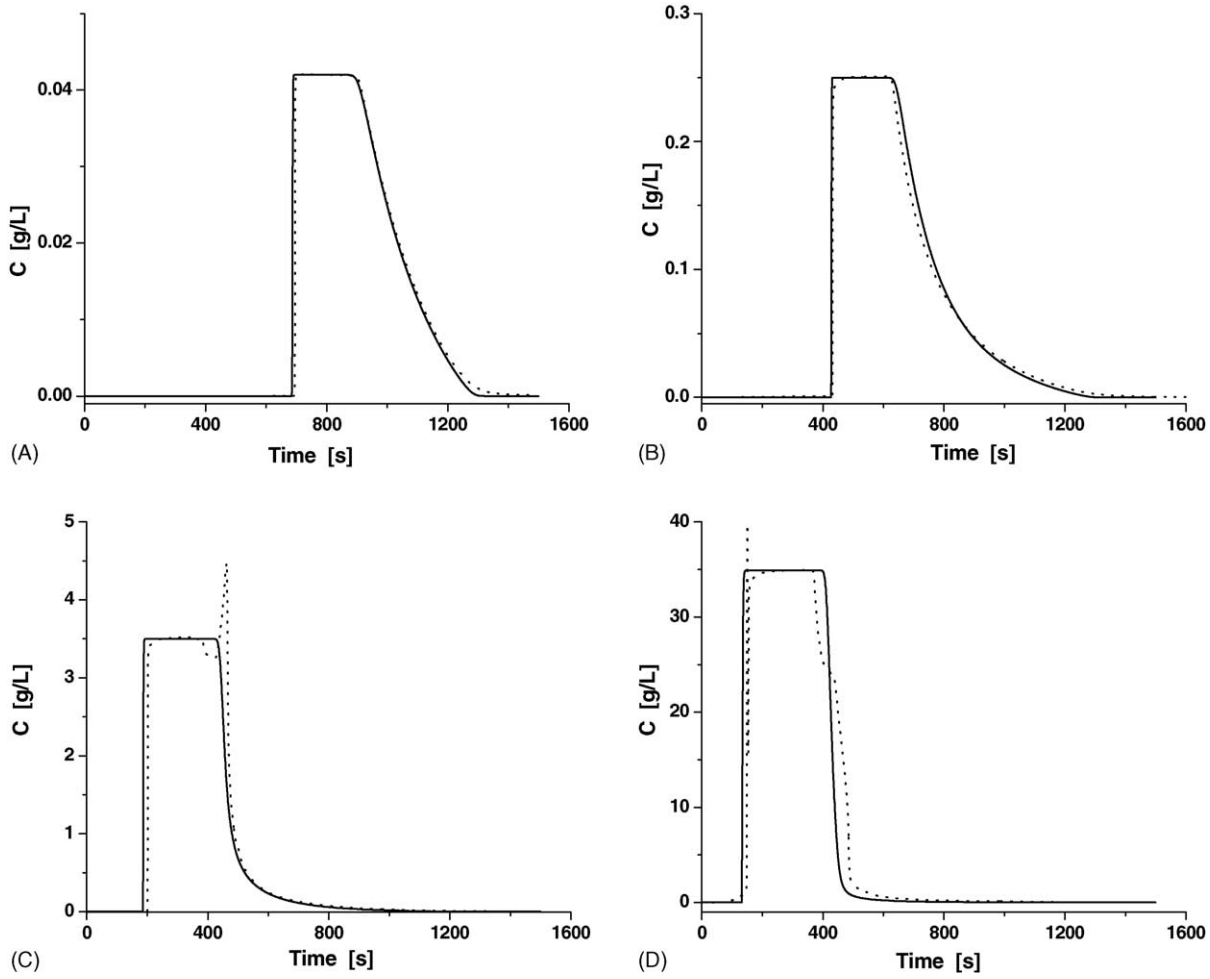

Fig. 10. Same as in Fig. 3 except for the isotherm parameters of nortriptyline used in the calculations are those derived from the competitive two-component adsorption data (Table 2).

the physical properties of the C_{18}-Discovery column (Table 1) and assuming a density of 2 g/L for the solid adsorbent, it is straightforward to derive from the saturation capacities obtained for the three types of sites, that there is one site of type 1 for 1.84 C_{18}-bonded chain, one site of type 2 for 23 C_{18}-bonded chains, and one site of type 3 for 154 bonded chains, assuming that one site can accommodate one molecule of either nortriptyline or amytriptyline. A C_{18}-bonded chain on the Discovery column occupies an average surface area of 55 $Å^2$. The surface area occupied by a molecule of nortriptyline or amytriptyline would be about 100 $Å^2$, which corresponds well to the molecular size of the hydrophobic core of these analytes. Then the formation of a dense, complete monolayer should be expected at saturation of the surface. Similarly, the average surface area occupied by a molecule of these compounds on sites of type 2 is 1265 $Å^2$, much larger than the molecular size. The average distance between two close sites of type 2 is about 50 Å. Finally, the same reasoning suggests that the average distance between two close sites of type 3 is about 130 Å. These distances are large and give an idea of the possible distribution of the surface heterogeneity of the C_{18}-bonded layer.

4.3. Production rate: production of pure nortriptyline (purity > 99.9%)

The separation of nortriptyline and amytriptyline cannot be achieved at very high concentrations because the low-energy sites are not selective enough. The breakthrough curves, shown in Fig. 8F–I, demonstrate experimentally an increasingly difficult separation when the concentration becomes larger than 0.2 g/L (0.1 g/L of each compound). The separation of the fronts of the individual profiles becomes poor. The axial dispersion of the individual band profiles and their poor resolution precludes the elution of pure nortriptyline. It is experimentally impossible to collect a significant fraction of pure nortriptyline (minimum collection time, $\Delta t = 5$ s, e.g. five droplets at 1 mL/min or almost 100 μL) in frontal analysis with a 0.2 g/L solution. The maximum concentration for which the separation of the two compounds can give a finite production is about 0.1 g/L. The most abundant type-1 sites cannot recognize the difference of only one methylene group between the two compounds studied. Yet, the presence of these sites is crucial for the production rate in preparative chromatography.

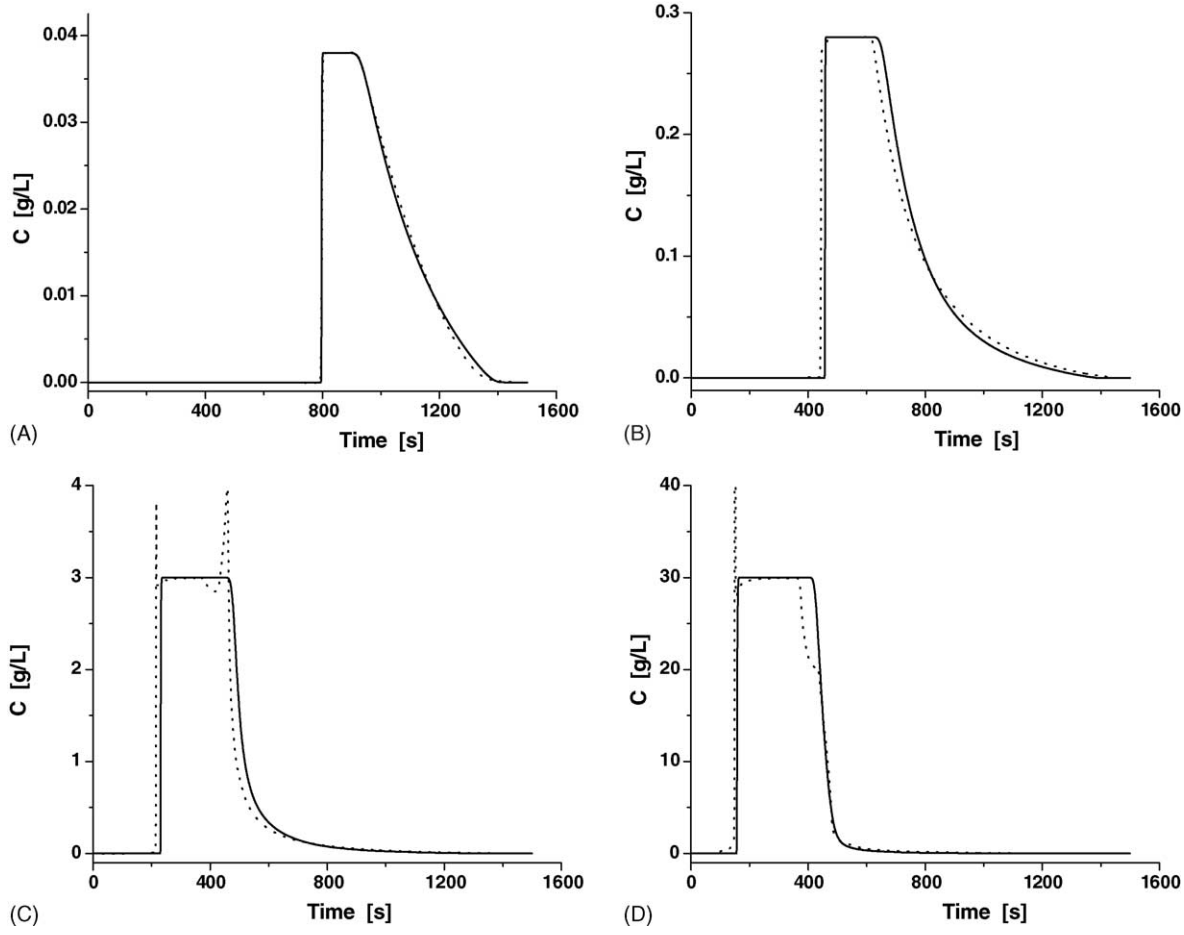

Fig. 11. Same as in Fig. 10 except for the compound amytriptyline.

On the other hand, the sites of type 3 are highly selective but are few. The separation of nortriptyline and amytriptyline is possible if not easy at low concentrations, which is not very practical from the preparative point of view. Only low production rates should be expected. For instance, the injections of 100 and 200 μL of a solution mixture at 1 g/L (0.5 g/L each) results in elution bands with a concentration at the column outlet lower than 0.1 g/L. Fractions were collected during the elution of these band profiles and reinjected. Fig. 12A and B compare these experimental profiles and those calculated with the ED model ($N = 12000$). The agreement is very good but is not perfect because each fraction was collected during 0.3 min (16 droplets at 1 mL/min), hence some degree of back-mixing is introduced. The concentration shocks observed at the head of the bands are not as sharp as those calculated. Based on the results of the calculations and using the actual column efficiency ($N = 12\,000$), it should be possible to collect pure nortriptyline (purity >99.9%) by ending the collection at 10.84 and 9.13 min for injections of 100 and 200 μL, respectively. The collection of pure amytriptyline (purity >99.9%) should begin at 14.69 and 14.81 min, respectively. The recovery yields Y_{Nor} and Y_{Ami} can be calculated as [1]

$$Y_i = \frac{n_i - A_i}{n_i} \tag{7}$$

where n_i is the amount of component i injected in the column and A_i is the amount of component i which eluted after the first cut point ($t_{c,1}$) for the less retained component or before the second cut point ($t_{c,2}$) for the more retained compound. Accordingly,

$$A_1 = F_v \int_0^{t_{c,1}} C_1 \, dt$$

and

$$A_2 = F_v \int_{t_{c,2}}^{\infty} C_2 dt$$

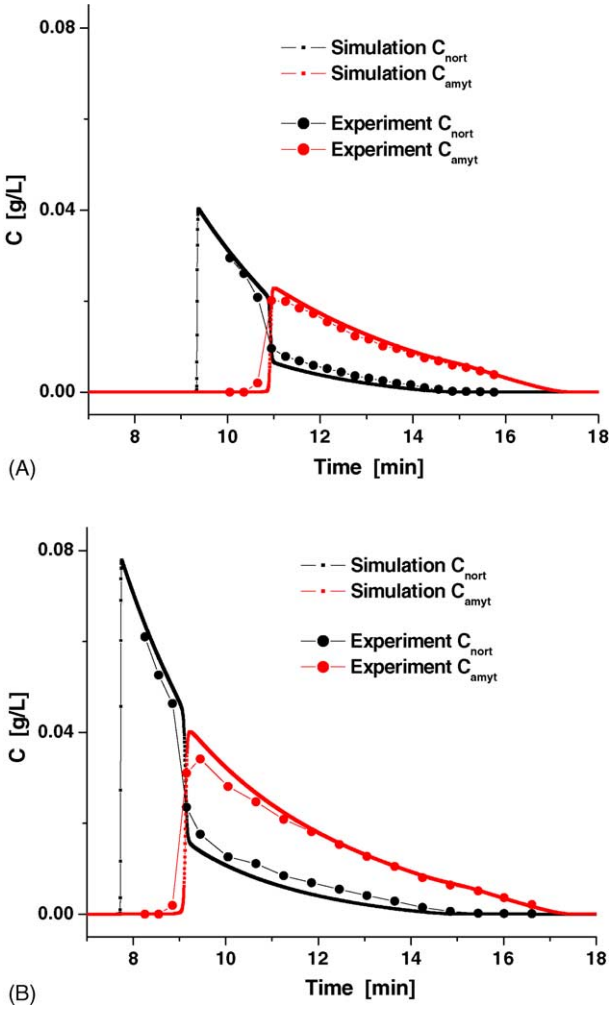

Fig. 12. Comparison between the simulated (ED model, $N = 12{,}000$) and experimental (by fraction collection and reinjection) individual band profiles of nortriptyline and amytriptyline. Same experimental conditions as in (A) Fig. 9G and (B) Fig. 9H.

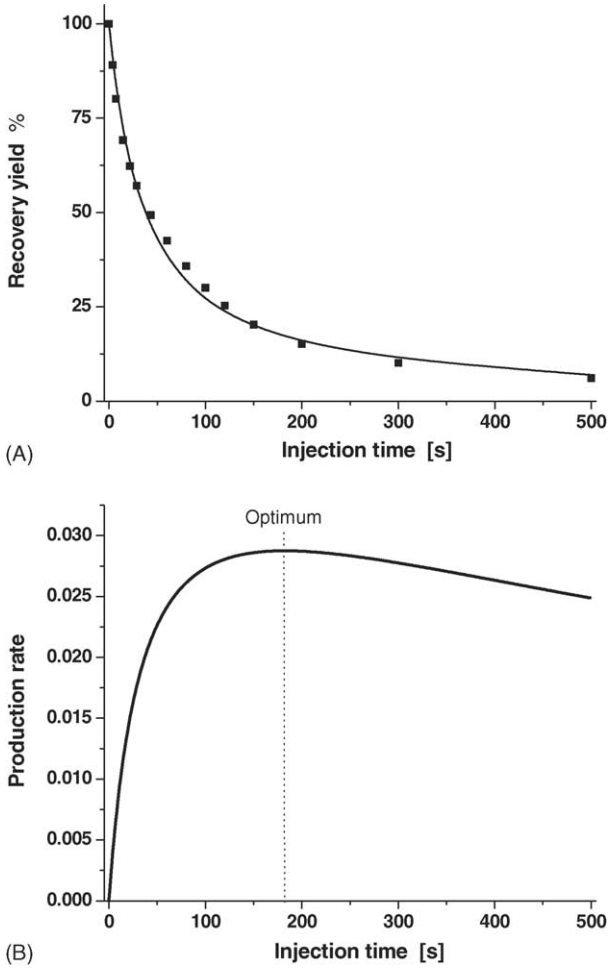

Fig. 13. Effect of the time of injection on the recovery yield (A) and production rate (B, arbitary unit) of nortriptytline. A purity of 99.9% was required. Flow rate 1 mL/min, $C_{nort} = 0.4754$ g/L, $C_{amyt} = 0.51$ g/L.

Note that because of the tag-along effect of component 1 (nortriptyline), the actual purity of the elution band of amytriptyline is low and only very few fractions of pure amytriptyline can be collected. This system is certainly not appropriate rapidly to produce significant amounts of pure amytriptyline.

When the concentrations of the two compounds are equal in the feed mixture, the recovery yield of nortriptyline is 80.1 and 69.2% when the injection times, t_{inj}, of a 1 g/L solution are 7.2 and 14.4 s, respectively. The larger the injection time, the lower the recovery yield because the distance between the two front shocks decreases and the quantity of lost feed increases. Fig. 13A shows how the recovery yield of nortriptyline decreases with increasing injection time, up to 500 s. Because the efficiency of the Discovery column is very good, the curve obtained is close to the ideal recovery that would correspond to an infinite column efficiency. The duration of one cycle is calculated by adding the corrected retention time of the most retained compound ($t_{R_2} - t_0 = k'_2 t_0$) and the injection time t_{inj}. The production rate Pr or amount of feed turned into product (e.g. purified compound at the required degree of purity) per unit time is given by

$$\mathrm{Pr} = \frac{Y(t_{inj}) F_v t_{inj} C_i^0}{k'_2 t_0 + t_{inj}} \tag{8}$$

The recovery yield can be fitted to a simple one-parameter decay function (Fig. 13A)

$$Y(t_{inj}) = \frac{1}{1 + 0.02689\, t_{inj}} \tag{9}$$

If we consider $F_v = 1\,\mathrm{mL/min} = 0.0167 \times 10^{-3}\,\mathrm{L/s}$ as an optimal flow rate ($N = 12000$), the optimal injection time is obtained by maximizing the production rate with respect to the injection time, only. The other parameters are $k'_2 t_0 = 892\,\mathrm{s}$ and $C_i^0 = 0.4754\,\mathrm{g/L}$.

The highest production rate is obtained for an injection that lasted 181 s (Fig. 13B). Then, 2.28×10^{-7} g of pure nortriptyline (>99.9%) can be produced per second with a single analytical Discovery column (containing about 1 g of packing material). A 2 in (5 cm) i.d. column would produce about 2.4 g of pure nortryptiline per day. This is a low production rate and this is due to the low number of selective sites on the column ($q_{s,2} + q_{s,3}$) representing barely a few percent of the total available surface area. Preparative chromatography requires as many selective sites as possible. Classical RPLC packing material are not the most appropriate packing material for this separation.

5. Conclusion

This work demonstrates how the acquisition of adsorption data using the FA method followed by the modeling of these data and the calculation of the AED permits a considerably improved understanding of the retention and separation mechanisms in HPLC. A considerable amount of information (distribution of the adsorption sites, saturation capacities and equilibrium constants of the types of sites identified, and possibly adsorbate-adsorbate interactions) is derived from these thermodynamic data. This information cannot be obtained using "linear chromatographic methods." The amount of compounds injected in the column with these methods must be a fraction of 1% of the saturation capacity of the adsorption sites of highest energy. The only data measured, the overall retention factor is biased in favor of the high energy sites, which are the first occupied although, by far, the least abundant. It does not provide any direct information on the homogeneity of the surface of packing materials. Thus, it leads to erroneous conclusions, as described elsewhere [13]. The separation scientist should be aware of the degree of heterogeneity of the adsorbent used and of the relative importance of the different types of sites to the properties of the material used, either for analytical or for preparative purposes.

In analytical applications, the retention of analytes at very low concentrations is governed by the properties of the high-energy adsorption sites, the first occupied. If these sites are few and have an energy markedly higher than lower energy types of sites, significant peak tailing takes place when large samples are injected for the analysis of trace or minor components [30,31]. Only the modeling of adsorption data and the calculation of the adsorption energy distribution can give clear conclusions regarding the heterogeneity of the adsorbent surface [13]. The fact that nortriptyline and amytriptyline compete for access to the high energy sites confirm that these are no artefacts.

For preparative applications, the heterogeneity of the adsorbent surface is also important. Although the surface area of low energy sites is much larger than that of the high energy sites, these latter sites are occupied first and liberated last, on the tail of bands. The corresponding term in the composite isotherms contributes considerably to enhance the tag-along effect and limits the production rate of purified compounds that can be achieved (see earlier). Furthermore, high energy sites are usually more selective than low energy sites.

All the conventional RPLC packing materials that we have studied are definitely heterogeneous [11,13]. For the lack of the proper tools and methods, this drawback has not yet been fully realized. Peak tailing is blamed on silanophilic interactions. It is probable that the high energy sites are due to silanol groups buried under the bonded alkyl chains but the presence of the intermediate energy sites has remained ignored until now. Besides, no quantitative estimates of the density of these sites nor of the differences between the average energies of each types of sites has been provided yet. The methods described here provide the means needed to characterize the heterogeneity of old or new packing materials and to follow and quantify rapidly the improvements that changes in their manufacturing process may bring. Obviously, the results obtained depend both on the morphology and chemistry of the surface but also on the size and chemical functionalities of

the probe used. Several probes will be needed and it is not sure that any of those that we have chosen are best.

Reducing the heterogeneity of the surface of chemically bonded silicas constitutes a great challenge for manufacturers. Yet, at this stage of development of chromatographic methods, manufacturing more homogeneous surfaces will be more useful for the community at large than merely increasing the column efficiency. It is critical in preparative chromatography. It would be extremely useful for many clinical and biochemical analyses.

Acknowledgments

This work was supported in part by grant CHE-02-44693 of the National Science Foundation, by Grant DE-FG05-88-ER-13869 of the US Department of Energy, and by the cooperative agreement between the University of Tennessee and the Oak Ridge National Laboratory.

References

[1] G. Guiochon, S.G. Shirazi, A.M. Katti, Fundamentals of Preparative and Nonlinear Chromatography, Academic Press, Boston, MA, 1994.
[2] H. Kim, F. Gritti, G. Guiochon, J. Chromatogr. A 1049 (2004) 25.
[3] X. Liu, D. Zhou, P. Szabelski, G. Guiochon, Anal. Chem. 75 (2003) 3999.
[4] F. Gritti, G. Guiochon, J. Chromatogr. A 995 (2003) 37.
[5] F. Gritti, G. Guiochon, J. Chromatogr. A 1033 (2004) 43.
[6] F. Gritti, G. Guiochon, J. Chromatogr. A 1033 (2004) 57.
[7] F. Gritti, G. Guiochon, J. Chromatogr. A 1047 (2004) 33.
[8] F. Gritti, G. Guiochon, Anal. Chem. 76 (2004) 4779.
[9] F. Gritti, G. Guiochon, J. Chromatogr. A 1038 (2004) 53.
[10] F. Gritti, G. Guiochon, J. Chromatogr. A 1041 (2004) 63.
[11] F. Gritti, G. Guiochon, Anal. Chem. 75 (2003) 5738.
[12] M. Rai, M. Herold, A. Ellwanger, G. Günter Gauglitz, K. Albert, Macromol. Chem. Phys. 201 (2000) 825.
[13] F. Gritti, G. Guiochon, Anal. Chem. 77 (2005) 1020.
[14] B. Lin, G. Guiochon, Modeling for Preparative Chromatography, Elsevier, Amsterdam, The Netherlands, 2003.
[15] O. Lisec, P. Hugo, A. Seidel-Morgenstern, J. Chromatogr. A 908 (2001) 934.
[16] J. Jacobson, J.H. Frenz, Cs. Horváth, Ind. Eng. Chem. Res. 908 (2001) 934.
[17] P. Forssén, J. Lindholm, T. Fornstedt, J. Chromatogr. A. 991 (2003) 31.
[18] D.W. Marquardt, J. Soc. Appl. Math. 11 (1963) 431.
[19] M. Jaroniec, R. Madey, Physical Adsorption on Heterogeneous Solids, Elsevier, Amsterdam, The Netherlands, 1988.
[20] B.J. Stanley, S.E. Bialkowski, D.B. Marshall, Anal. Chem. 65 (1993) 259.
[21] D.M. Ruthven, Principles of Adsorption and Adsorption Processes, Wiley, New York, NY, 1984.
[22] M. Suzuki, Adsorption Engineering, Elsevier, Amsterdam, The Netherlands, 1990.
[23] F. Gritti, G. Guiochon, J. Chromatogr. A 1003 (2003) 43.
[24] F. Gritti, G. Guiochon, J. Chromatogr. A 1028 (2004) 105.
[25] F. Gritti, G. Guiochon, J. Chromatogr. A, submitted for publication (f38).
[26] A. Méndez, E. Bosch, M. Rosés, U.D. Neue, J. Chromatogr. A 986 (2003) 33.
[27] U. D. Neue, K. Van Tran, A. Méndez, P. W. Carr, J. Chromatogr. A.
[28] F. Gritti, G. Guiochon, J. Chromatogr. A 1053 (2004) 59.
[29] F. Gritti, G. Guiochon, Anal. Chem. 77 (2005) 4257.
[30] D.V. McCalley, J. Chromatogr. A 738 (1996) 169.
[31] D.V. McCalley, Anal. Chem. 75 (2003) 3404.